up to 200 km away. Also, wind patterns and the wake region behind each slug will have a major influence on the path of the slugs. At high repetition rates it is anticipated that slug passage through the atmosphere will be beneficially affected. However, for this concept to work the impact diameter at the vehicle must be held to approximately 10 m. Some maneuvering by the vehicle is acceptable for gross changes in the slug stream, but if the slugs arrive with a large random dispersion, the vehicle will not be able to respond to the individual slugs. Further work is needed on this subject.

The final factor considered here is the possibility that either kinetic energy or some form of chemical energy carried by the slugs can be put to use. If the kinetic energy of the arriving mass could be converted directly into thermal energy upon collision, the vapor thus formed could be harnessed to provide propulsive thrust to the ascending vehicle. For example, a relative velocity of 2 km/s represents an enthalpic value of 2 MJ per kilogram of slug. For slug material composed primarily of water, this enthalpic value is approximately the heat of vaporization at standard pressure. If we go one step further, perhaps a monopropellant cryogenically frozen into a solid form would provide a suitable material that would either burn or detonate on impact. With such a configuration, the scheme proposed here begins to look like a chemically driven Orion-type vehicle relying on a ground-based mass driver for propellant delivery. These interesting variations on the basic concept can be seriously considered once the major question on slug passage through the atmosphere has been resolved.

References

[1]Hawke, R. S., Brooks, A. L., Fowler, C. M., and Peterson, D. R., "Electromagnetic Railgun Launchers: Direct Launch Feasibility," *AIAA Journal*, Vol. 20, No. 7, 1982, pp. 978–985.

[2]Wilbur, P. J., Mitchell, C. E., and Shaw, B. D., "The Electrothermal Ramjet," *AIAA Journal*, Vol. 20, No. 6, 1983, pp. 603–610.

[3]Jones, G. R., Swanson, N. J., Madura, D. L., and Bohannon, R. C., "Aerothermodynamic Issues Associated with Rail Gun Launched to Space Projectiles," AIAA Paper 90-1720, June 1990.

[4]Singer, C. E., "Interstellar Propulsion Using a Pellet Stream for Momentum Transfer," *Journal of the British Interplanetary Society*, Vol. 33, No. 3, 1980, pp. 107–115.

[5]Rupp, H. O., "Comments on 'Interstellar Propulsion Using a Pellet Stream for Momentum Transfer' by C. E. Singer," *Journal of the British Interplanetary Society*, Vol. 34, No. 3, 1981, pp. 115–116.

Effect of Transverse Vibration on the Performance of a Heat Pipe

Mark C. Charlton* and W. Jerry Bowman†
Air Force Institute of Technology,
Wright-Patterson Air Force Base, Ohio 45433

Introduction

THE growing number of current and potential applications for heat pipes brings with it an expanding set of environmental conditions under which the heat pipe must function. This research is a step toward evaluating what effect, if any, these environmental conditions have on the capabilities of heat pipes. In particular, this experiment examined how a heat pipe might operate in an environment where it is subjected to vibration.

Received May 28, 1993; presented as Paper 93-2734 at the AIAA 28th Thermophysics Conference, Orlando, FL, July 6–9, 1993; revision received Sept. 25, 1993; accepted for publication Oct. 4, 1993.

*Graduate Student.

†Associate Professor of Aerospace Engineering. Senior Member AIAA.

A literature search revealed that little research has been done on the effects of vibration on heat pipe performance. Deverall[1] reported on an experiment designed to evaluate the effect of vibration on a heat pipe. The conclusion to this report is that "sinusoidal and random vibration, within the spectrum tested, are not detrimental to heat pipe performance." A second work addressing this subject was a report by Richardson et al.[2] They investigated the effect of longitudinal vibration on heat pipe performance. It was reported that the effect is greater at lower frequencies and higher amplitudes. The authors indicated that "the most pressing need is for an investigation providing information on actual maximum heat transfer capability" and that "an investigation should be made of the effect of transverse vibration."

The objective of this research is to determine the effect of transverse vibration on the capillary limit of a heat pipe. To attain this objective, an experimental heat pipe and apparatus were designed and built. The static performance of the pipe was first measured through a series of tests with no vibration input. These tests provided a baseline of maximum heat transport for the pipe over a range of heat pipe operating temperatures. Once this baseline performance was established, tests were run with vibration input perpendicular to the longitudinal axis of the pipe. The results from the vibration test runs were compared to those from the static baseline runs to determine if there was any effect on the maximum heat transport due to transverse vibration.

Experiment Design

The heat pipe used during the experiment was constructed of oxygen-free hard copper. It consisted of a section of pipe 0.3175 m in length to allow for a 0.3048-m total working length after installation of the endcaps, each of which had a total depth of 0.6350 cm. The outside diameter of the pipe was 2.223 cm and the inside diameter was 1.892 cm. The wall thickness was 1.651 mm. It had a condenser section 0.1111 m long, an adiabatic section 0.09210 m long, and an evaporator section 0.1016 m long. Fig. 1 is an illustration of the pipe.

The wick was constructed of 100-mesh copper screen. It had a length of 0.3048 m and a width of .01191 m to allow for two complete wraps of screen. 5.7 g of water were inserted into the heat pipe as the working fluid. All parts were given a final cleaning before assembly, closing, and filling of the pipe. The cleaning and fill process are discussed in detail in Ref. 3.

A flexible tape heater was used to heat the evaporator end of the heat pipe. This heater had a length of 1.829 m and a width of 1.270 cm. The maximum power of the heater was 470 W at 120 V, and it had a power density of 2.015×10^4 W/m^2. With an evaporator section length of only 0.1016 m, the heater was wrapped in layers in order to get sufficient power density to run the experiment. The heater was insulated. This is turn was covered with an aluminum foil adhesive tape to hold the batting together during vibration. The electrical power input to the heater was monitored using a voltmeter and an ammeter.

A coolant control system was required in order to operate the pipe at various temperatures. While the pipe was operating in the heat pipe mode, the pipe operating temperature could be varied by varying the condenser temperature. This was accomplished by changing the coolant flow rate. Normal tap water was used as a coolant and was run through the manifold surrounding the condenser section of the heat pipe. The coolant inlet temperature was not controlled and was determined by the temperature of the water in the building plumbing.

The data acquisition system for this experiment had to be capable of reading and storing vibration frequency and amplitude data, temperature data, heater power data, and coolant flow-rate data. The vibration data were measured using accelerometers. The vibration in the actuator axis direction was the control variable for the experiment, so it was at a known frequency and amplitude. The vibration frequency and amplitude in the other two directions were measured using single-axis accelerometers aligned with these axes and mounted on the vibration fixture. The output from the "off-axis" accelerometers was routed into an oscilloscope for display. The readings for the off-axis vibration amplitudes were taken man-

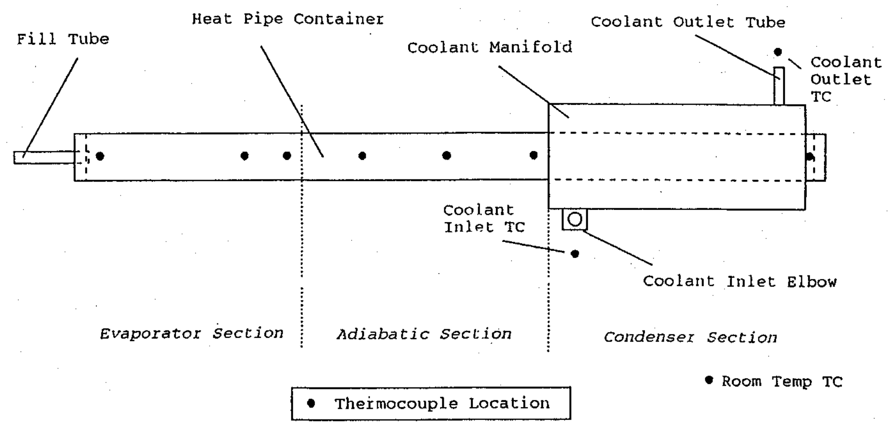

Fig. 1 Heat pipe tested.

ually from the oscilloscope. Temperature measurements were taken using T-type thermocouples. The 10 thermocouples used to measure temperatures were mounted as shown in Fig. 1.

Experimental Test Procedure

The experimental test procedure was developed over a series of preliminary runs and designed to provide repeatability and accurate data collection from test run to test run. The first step in the procedure was to ensure the heat pipe was at room temperature. The pipe was then tilted to an angle of approximately 45 deg (evaporator down). This ensured that the evaporator wick was completely wet. While inclined 45 deg, the heater power was set at 100 W. This mode of operation was maintained until the heat pipe operating temperature reached 35°C. The heat pipe operating temperature was taken to be the same as the pipe wall temperature in the adiabatic section. Once on operating temperature of 35°C was reached, the pipe was leveled and the vibration level for that test run was set. The pipe was allowed to come to steady operation under this condition. The heater power was then increased in increments of 5 W until the evaporator section began to dry out. Evaporator dryout was indicated by a rapid increase in the temperature at the evaporator end of the pipe, and this was considered the failure condition for the test run.

Experimental Results

The static capillary limit was determined through a series of 29 experimental test runs, made at a wide range of operating temperatures from 42 to 102°C. These data represented a baseline to which performance runs could be compared.

Having established the baseline performance, the heat pipe performance in a vibration environment was measured. Several test runs were made at each frequency and amplitude combination to ensure that the data collected was repeatable. The three frequencies chosen were 30, 250, and 1000 Hz. This range was intended to address both the lower frequencies often present in mechanical machinery and also the higher frequencies found in more dynamic systems. The three vibration levels chosen were 1.0, 2.5, and 5.0 g. These, again, were chosen to represent likely loads to be experienced by a heat pipe as part of a system.

A sinusoidal input was used for each of the vibration tests. Measurement of the vibration level in the three orthogonal directions confirmed that vibration input to the pipe was primarily transverse vibration, with very little longitudinal vibration of the pipe. Vibration level was typically an order of magnitude less severe along the pipe longitudinal axis than in the transverse direction.

Once the static and the vibration data were collected, they were plotted for comparison. Figures 2 and 3 illustrate all of the vibration and static data collected. From these graphs it is clear that the majority of the data fall below the analytical model, but they follow the same basic trend as the prediction.

To examine the effect of each vibration level and frequency on the capillary limit, separate plots of each were created, and these are available in Ref. 3. An examination of these plots revealed that there was no evident effect that could be attributed to the vibration

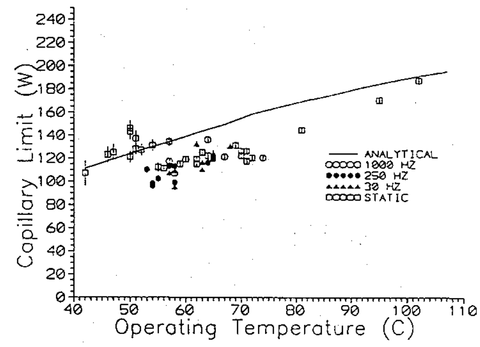

Fig. 2 Experimental data for different frequencies.

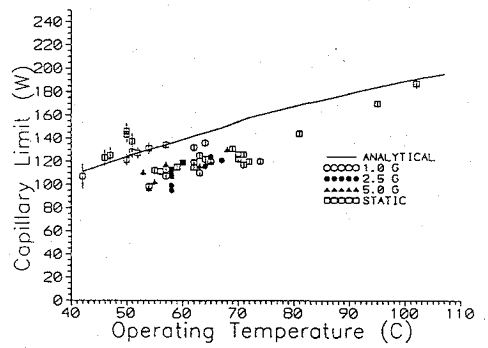

Fig. 3 Experimental data for different amplitudes.

level. Although a few of the data points were low compared to static points at similar temperatures, the majority were near or even above corresponding static results.

After evaluating the results according to vibration level, they were next plotted according to frequency of vibration. This representation of the results again gave several points where the capillary limit was lower than the corresponding static results; however, here again, there is no trend that encompasses a majority of the points except at a frequency of 250 Hz, where a slight degradation in performance might have occurred.

Conclusion

For this experiment, a heat pipe was designed, constructed, and then tested to determine what effect transverse vibration would have on its capillary limit. The heat pipe capillary limit was experimentally determined with no vibration input, and these static results were used as the baseline performance. The capillary limit was then reevaluated while the heat pipe was subjected to vibration.

The comparison of the results from the vibration testing with those from the static testing revealed that there was no significant effect on the capillary limit caused by transverse vibration. The 250 Hz test runs indicated what could be interpreted as a minimal degradation of the maximum heat transport rate; however, this finding was inconclusive. Although this conclusion can be strictly applied only to this pipe at the vibration frequencies and levels tested, it can be expected to be applicable to pipes of similar construction at levels of vibration near to those evaluated here.

References

[1]Deverall, J. E., "The Effect of Vibration on Heat Pipe Performance," Los Alamos Scientific Laboratory, Los Alamos, NM LA-3798, Oct. 1967.

[2]Richardson, J. W. et al., "The Effect of Longitudinal Vibration on Heat Pipe Performance," *Journal of Astronautical Sciences*, Vol. 17, No. 5, 1970, pp. 249–265.

[3]Charlton, M. C., and Bowman, W. J., "Effect of Transverse Vibration on the Capillary Limit of a Wrapped Screen Wick Copper/Water Heat Pipe," AIAA Paper No. 93–2734, July 1993.

Dynamical Instability of the Aerogravity Assist Maneuver

Colin R. McInnes*
University of Glasgow,
Glasgow G12 8QQ, Scotland, United Kingdom

Introduction

THE use of aerodynamic lift for the modification of conventional gravity-assist trajectories has recently been discussed as a means of enabling certain inner and outer solar-system missions.[1,2] Using a high-lift-to-drag vehicle, such as the waverider type,[3] trajectory bending angles far in excess of what may be obtained using ballistic gravity assist alone are attainable.

The aerogravity-assist (AGA) trajectory is essentially an equilibrium solution to the dynamical equations. With the vehicle in an inverted configuration, aerodynamic lift and the gravitational acceleration balance the normal acceleration due to trajectory curvature.

In this study the fundamental dynamical equations are used to form a single expression for the vertical acceleration. It is then demonstrated that for initial errors in altitude the resulting AGA trajectory is exponentially unstable. This may lead to the vehicle prematurely exiting the planetary atmosphere or impacting on the surface in some instances. It is however demonstrated that feedback linearization may be used to ensure stability and tracking of the required altitude for equilibrium flight.

Although there are many dynamical issues associated with the AGA maneuvre (e.g., atmospheric uncertainties), this analysis highlights the need for precise guidance, navigation, and control to ensure a successful atmospheric pass meeting the required exit conditions.

AGA Flight Dynamics

For ease of illustration the dynamical equations are formulated in a nonrotating wind-free atmosphere. The vehicle position is described by planetocentric polar coordinates (r, θ), and the vehicle motion is described by the inertial velocity v and flight-path angle γ, as shown in Fig. 1. In this analysis the vehicle uses the bank angle σ as a single control input for lift modulation, with the angle of attack trimmed for maximum lift. The two dynamical and two kinematic equations are therefore given by

$$\frac{\mathrm{d}v}{\mathrm{d}t} = -\frac{D}{m} + g\sin\gamma \tag{1a}$$

$$v\frac{\mathrm{d}\gamma}{\mathrm{d}t} = -\left(\frac{v^2}{r} - g\right)\cos\gamma - \frac{L}{m}\cos\sigma \tag{1b}$$

Received Oct. 10, 1992; revision received Dec. 15, 1992; accepted for publication Dec. 16, 1992.

*Department of Aerospace Engineering.

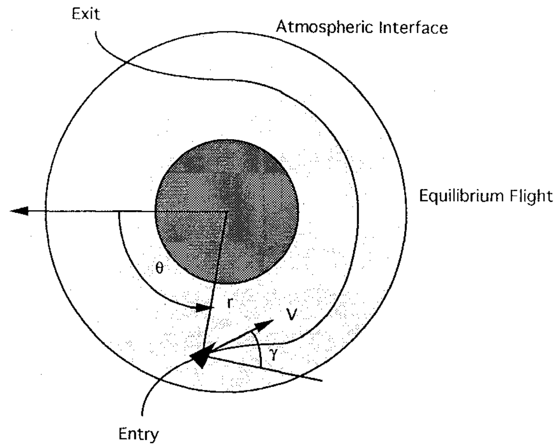

Fig. 1 Schematic geometry of the aerogravity assist maneuver.

$$\frac{\mathrm{d}r}{\mathrm{d}t} = -v\sin\gamma \tag{1c}$$

$$\frac{\mathrm{d}\theta}{\mathrm{d}t} = \frac{v}{r}\cos\gamma \tag{1d}$$

where g is the planetary gravitational acceleration. The aerodynamic lift and drag are defined in terms of the lift and drag coefficients C_L and C_D as

$$\begin{Bmatrix} L \\ D \end{Bmatrix} = \tfrac{1}{2}\rho(r)Sv^2\begin{Bmatrix} C_L \\ C_D \end{Bmatrix} \tag{2}$$

where S is the aerodynamic reference area and the atmospheric density ρ is assumed to be a function of altitude only.

Differentiating Eq. (1c) and substituting, an expression for the vertical acceleration may be derived as

$$\frac{\mathrm{d}^2r}{\mathrm{d}t^2} = \frac{v^2}{r}\cos^2\gamma - g + \frac{D}{m}\sin\gamma + \frac{L}{m}\cos\sigma\cos\gamma \tag{3}$$

For the AGA maneuver level, constant-altitude flight is required so that the left-hand side of Eq. (3) vanishes. Setting $\gamma = 0$, the required bank angle σ^* may then be obtained as

$$\sigma^* = \cos^{-1}\left[\frac{2m}{\rho(r)C_LS}\left(\frac{g}{v^2} - \frac{1}{r}\right)\right] \tag{4}$$

where $\pi/2 < \sigma^* < 3\pi/2$, as the vehicle must be oriented in an inverted configuration with the aerodynamic lift and gravity in equilibrium with the outward normal acceleration. Transverse motion may be eliminated by periodic roll reversals, unless there is a specific requirement for a plane change.

For the cases of interest with atmospheric entry at large hyperbolic velocities, the gravitational acceleration may be neglected with respect to the aerodynamic and normal accelerations. The required bank angle is then a function of altitude only.

Linear Stability Analysis

In order to investigate the stability of the AGA maneuver the vertical acceleration equation will be perturbed with the vehicle initial flight-path angle $\gamma_0 = 0$ and velocity v_0 fixed. Perturbing the vehicle altitude so that $r \to r_0 + \xi$ in Eq. (3) and retaining terms of order ξ, it is found that

$$\frac{\mathrm{d}^2\xi}{\mathrm{d}t^2} + \left[\frac{v^2}{r^2} + \frac{\rho'(r)}{\rho(r)}\left(\frac{v^2}{r} - g(r)\right) + g'(r)\right]_0 \xi + O(\xi^2) = 0 \tag{5}$$

where the required bank angle σ^* has been substituted from Eq. (4). This variational equation is of the standard form with solution $\xi(t)$, viz.,

$$\frac{\mathrm{d}^2\xi}{\mathrm{d}t^2} + \Lambda^2(v_0, r_0)\xi = 0 \to \xi(t) = \xi_{01}e^{-\sqrt{\Lambda^2}t} + \xi_{02}e^{-\sqrt{\Lambda^2}t} \tag{6}$$